Pliocene Indonesian Throughflow and Leeuwin Current dynamics: Implications for Indian Ocean polar heat flux

Cyrus Karas,[1,2] Dirk Nürnberg,[1] Ralf Tiedemann,[3] and Dieter Garbe-Schönberg[4]

[1]   To understand the gradual global cooling during the mid-Pliocene (3.5–2.5 Myr ago) one needs to consider the tectonical constriction of tropical seaways, which affected ocean circulation and the evolution of climate. Here we use paired measurements of $\delta^{18}O$ and Mg/Ca ratios of planktonic foraminifera to reconstruct the Pliocene hydrography of the western tropical Indian Ocean (Site 709C) and changes in the Leeuwin Current in the eastern subtropical Indian Ocean (Site 763A) in response to Indonesian Gateway dynamics. Today, the Indonesian Throughflow (ITF) and, subsequently, the warm southward flowing Leeuwin Current off Western Australia are essential for the polar heat transport in the Indian Ocean. During 3.5–3 Ma, sea surface temperatures significantly dropped in the Leeuwin Current area, becoming since ~3.3 Ma 2°C–3°C cooler than the rather unchanged sea surface temperatures from the eastern and western tropical Indian Ocean. We refer this drop in sea surface temperatures to a weakened Leeuwin Current with severe climatic effects on Western Australia induced by a tectonically reduced surface ITF. We suggest that this reduced surface ITF led to a diminished poleward heat transport in the Indian Ocean resulting in a weakened Leeuwin Current and possibly to cooling of the Benguela upwelling system.

1.   Introduction

[2]   During the mid-Pliocene, earth gradually changed from greenhouse with globally warmer temperatures and minor ice coverage at high northern latitudes to icehouse with the prominent Northern Hemisphere Glaciation and the extension of continental ice sheets [*Ravelo et al.*, 2004; *Mudelsee and Raymo*, 2005]. This climate transition was accompanied by a main tectonic reorganization of the Indonesian Gateway triggering a change in the throughflow from initially South Pacific to North Pacific subsurface waters as indicated by a significant cooling at subsurface levels in the tropical eastern Indian Ocean [*Cane and Molnar*, 2001; *Karas et al.*, 2009]. A tectonically induced effect on the meridional heat transport toward the Southern Hemisphere was not yet proven, although today the Indonesian Throughflow (ITF) is assumed to be responsible for the largest poleward heat flux of ~0.59 PW (1 PW = 10^{15} W) in the Southern Ocean

[*Talley*, 2003; *Gordon*, 2005]. The Leeuwin Current, which is an important branch of the poleward heat transport in the Indian Ocean, is mainly drawn from the ITF [*Feng et al.*, 2003]. At modern conditions the Leeuwin Current transports up to 5 Sverdrups (1 Sverdrup = $10^6 \, \text{m}^3 \, \text{s}^{-1}$) of relatively warm and less saline tropical waters in the upper 200–250 m from the ITF region southward along the west coast of Australia, predominantly against equatorward winds (Figure 1) [*Smith et al.*, 1991]. It thereby suppresses coastal upwelling [*Morrow et al.*, 2003] and leads to distinctly warmer sea surface temperatures (SST) than at any other subtropical eastern boundary zone commonly characterized by strong upwelling.

[3]   We here present combined planktonic foraminiferal Mg/Ca and $\delta^{18}O$ data spanning the time period from 6 to 2 Ma from ODP sites 763A in the subtropical eastern Indian Ocean within the present influence of the Leeuwin Current (20° 35.20′S, 112°12.50′E, 1367 m water depth; Figure 1) and 709C (03°54.9′S, 60°33.1′E, 3041 m water depth; Figure 1) in the tropical western Indian Ocean (isotope data from *Shackleton and Hall* [1990]). We used the combined $\delta^{18}O$- and Mg/Ca-derived temperatures from Site 763A to calculate $\delta^{18}O$ of seawater that approximate changes in ancient salinities (see section 2.4). The analysis of the surface dwelling planktonic foraminifera *Globigerinoides sacculifer* allow us

[1]Leibniz Institute of Marine Sciences (IFM-GEOMAR), University of Kiel, Kiel, Germany.
[2]Goethe-University Frankfurt, Frankfurt am Main, Germany.
[3]Alfred Wegener Institute for Polar and Marine Research, Bremerhaven, Germany.
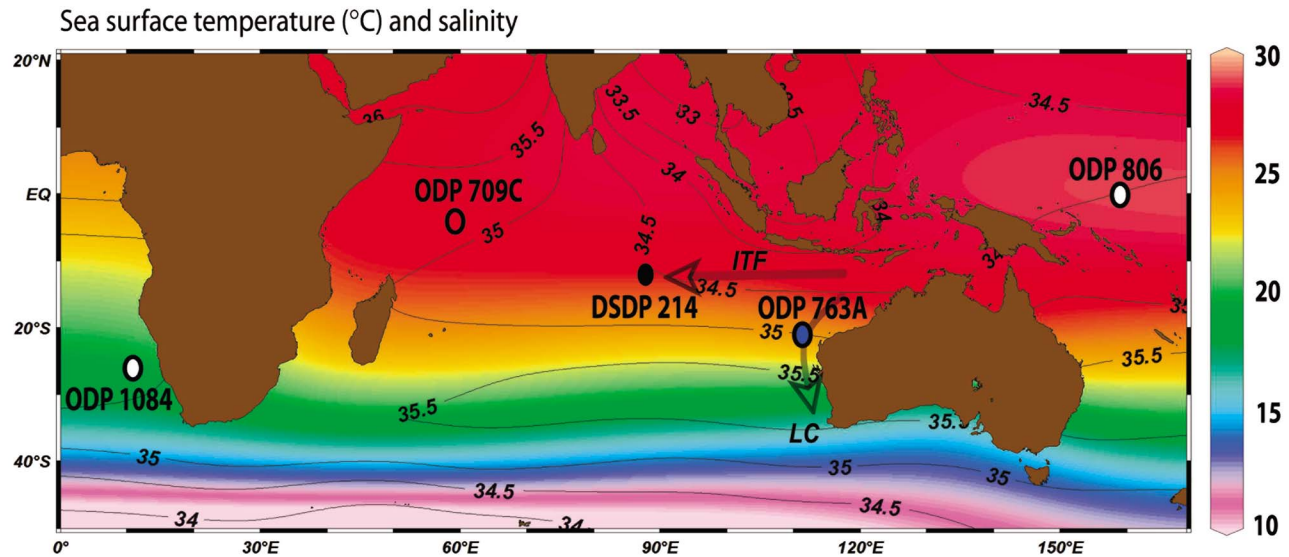[4]Institute of Geosciences, University of Kiel, Kiel, Germany.

Figure 1. Chart of annual ocean temperatures (color shading, degrees Celsius) and salinities (contour lines) at 20 m water depth [*Locarnini et al.*, 2006; *Antonov et al.*, 2006]. Paleoceanographic proxy data were generated for ODP Sites 763A and 709C. The pathways of the Indonesian Throughflow (ITF) and Leeuwin Current (LC) and locations of sediment cores discussed in the text are indicated.

to monitor changes in the surface near Leeuwin Current compared to the Indo-Pacific Warm Pool.

2. Materials and Methods

2.1. Age Models of Studied DSDP/ODP Sites

2.1.1. Site 709C

[4] To improve the initial age control from *Shackleton and Hall* [1990], we tuned the adjusted *G. ruber/G. sacculifer* δ^{18}O record (see section 2.2) [*Shackleton and Hall*, 1990] to the *G. sacculifer* δ^{18}O record of Site 806 [*Wara et al.*, 2005] using Analyseries 1.2 [*Paillard et al.*, 1996] (Figure 2a). Our tuning is thereby based on the graphical correlation between both records with linear integration between single tuning points. We selected Site 806 as a reference for tuning due to the following reasons. First, as both sites lie within the Indo-Pacific Warm Pool, we assume a similar development of both δ^{18}O signals over time. Second, the resolution of the *G. sacculifer* δ^{18}O record of Site 806 is high enough (~8 kyr) to serve as a tuning reference. Third, the initial age model of Site 806 used by *Wara et al.* [2005] was improved by *Karas et al.* [2009], by tuning the high-resolution benthic δ^{18}O record (4–2 Ma) to the LR04 stack [*Lisiecki and Raymo*, 2005]. The correlation between both δ^{18}O records is 0.6 (after removal of linear trend and mean). The resulting depth-age relationship is supported by the good fit with the nannofossil biodatums (maximum deviation of <1 m, or <100 kyr) reported by *Shackleton and Hall* [1990], the ages of which were updated to the ATNTS 2004 time scale (Figure 2b) [*Lourens et al.*, 2004]. Therefore, the combined use of tuning of the planktonic isotope record to Site 806 and well constrained nannofossil biodatums produces a reliable age model for Site 709C.

2.1.2. Site 763A

[5] For an initial age control of Site 763A, we selected those magnetic reversal ages (depths from *Tang* [1992]; ages were updated to the ATNTS 2004 time scale [*Lourens et al.* 2004]), which lie on the already established depth-age plot for this site [*Sinha and Singh*, 2008]. To further improve the age model especially during the critical time period 3.5–3 Ma, we generated a high-resolution (~5.5 kyr) benthic δ^{18}O (*Cibicidoides wuellerstorfi*) record for the interval ~3.8–3.1 Ma, which was then fine tuned to the LR04 stack (Figure 3a) [*Lisiecki and Raymo*, 2005]. The correlation between records is 0.7. To further check the established stratigraphy during 3.8–3.1 Ma, we performed astronomical tuning. The obliquity (41 kyr) filtered component of the benthic δ^{18}O record is in accordance to the obliquity solution of *Laskar* [1990] (Figure 3b) supporting our age model. We observed and corrected for a phase lag of ~8 kyr between obliquity and obliquity-controlled variations in the benthic δ^{18}O record. This phase lag is thought to be relatively constant and is linked to climatic processes in the high latitudes [e.g., *Tiedemann et al.*, 2007]. The resulting depth-age curve for the entire time period studied matches the magnetic reversal ages (Figure 3c).

2.2. Mg/Ca and δ^{18}O Analysis

[6] For stable oxygen isotope and Mg/Ca analyses, ~30 specimens were selected from shallow dwelling planktonic foraminifera *G. sacculifer* (without sac-like chamber). Only in a few cases, the number had to be reduced to ~10 specimens. Specimens were selected from the 315–355 μm size fraction to avoid size effects in δ^{18}O values and Mg/Ca [*Elderfield et al.*, 2002]. The size fraction had to be widened to the 315–400 μm size fraction when only insufficient foraminiferal tests were within the narrow fraction. Subsequently, sample material was gently crushed, mixed
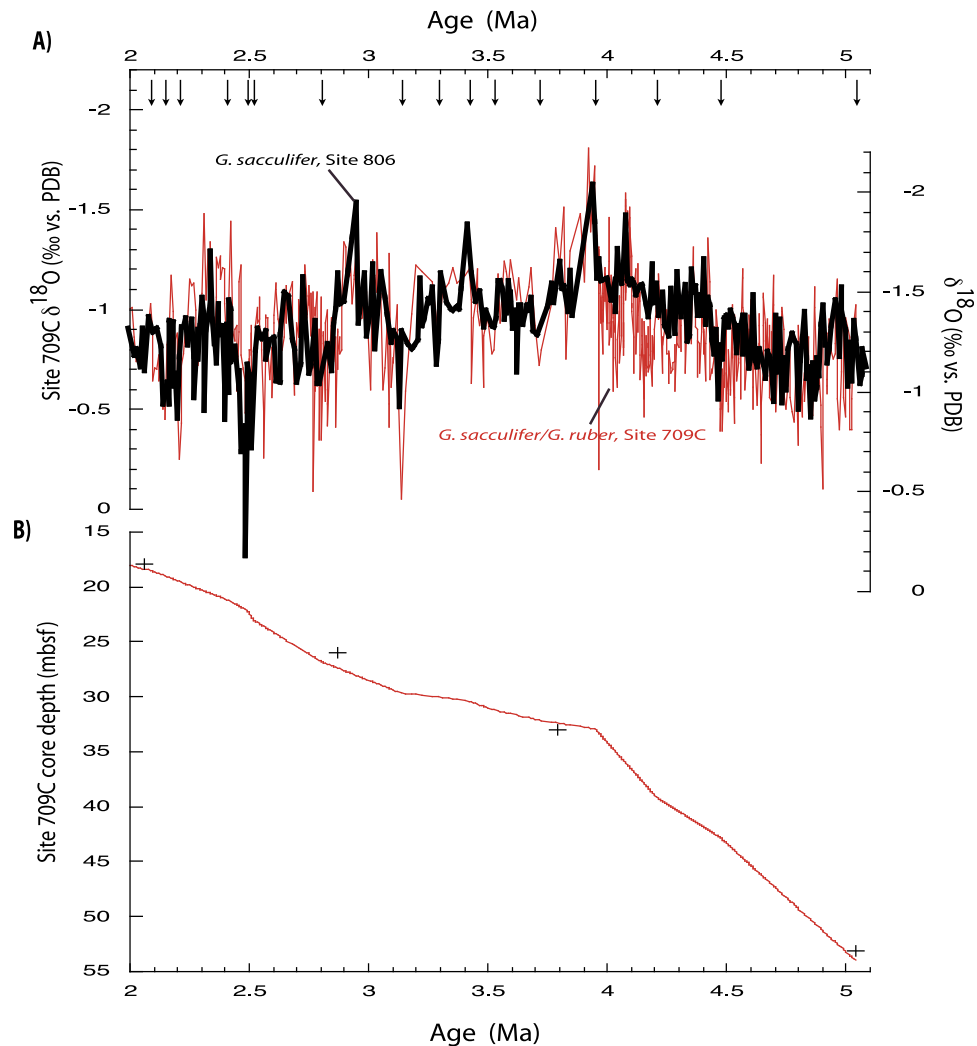
Figure 2. Revised stratigraphic framework of Site 709C. (a) Tuning of the high-resolution planktonic *G. ruber*/*G. sacculifer* $\delta^{18}O$ record (red line; *G. ruber* values were adjusted to *G. sacculifer*) [*Shackleton and Hall*, 1990] to the *G. sacculifer* $\delta^{18}O$ record of Site 806 (black line) [*Wara et al.*, 2005]. Arrows indicate tie points. (b) Diagram showing the age-depth relationship of Site 709C (red line). Nannofossil datums [*Shackleton and Hall*, 1990] are indicated (black crosses).

and divided into two thirds used for Mg/Ca analyses, and one third for stable isotope measurements. Isotope measurements were either conducted on a Finnigan MAT-252 (at IFM-GEOMAR, Kiel) or on a Finnigan MAT-251 mass spectrometer (at the Leibniz-Laboratory for Radiometric Dating and Stable Isotope Research, Kiel), both equipped with a fully automated carbonate preparation device. Both machines had an analytical precession better than ±0.07‰ for $\delta^{18}O$ (±1σ). All values are reported relative to Pee Dee Belemnite (PDB, based on calibration directly to National Bureau of Standards, NBS-19). From Site 709C, we used the published $\delta^{18}O$ record from *Shackleton and Hall* [1990], who selected in the older part of the core (>4 Ma) *G. sacculifer* and in the younger part *G. ruber* specimens. In order to make the $\delta^{18}O$ values from both species comparable, we added 0.25‰ to the $\delta^{18}O_{G.\ ruber}$ record, being consistent to studies at the same site [*Shackleton and Hall*, 1990] and in the tropical eastern Indian Ocean Site 214 [*Karas et al.*, 2009].

[7] For Mg/Ca analyses, foraminiferal tests were cleaned according to the established cleaning protocol of *Barker et al.* [2003] (nonreductive) in accordance to previously published Mg/Ca data from Site 214 used for comparison [*Karas et al.*, 2009]. Measurements were performed on a simultaneous, radially viewing ICP-OES (Ciros CCD SOP, Spectro A.I., Germany, Institute of Geosciences, University of Kiel). The analytical error for the Mg/Ca ratios is ~0.17%. Replicate analysis of the same samples, cleaned and analyzed during different sessions, show a standard deviation of <0.1 mmol/mol (relative standard deviation < 3%). Monitoring of Fe/Ca and Mn/Ca indicated that contamination with clays or Mn carbonates after cleaning was not an issue. Fe/Mg values are commonly significantly lower than 0.1 mmol/mol indicative for negligible contamination by silicate phases [*Barker et al.*, 2003]. Only at Site 763A we rejected 8 samples, as Fe/Mg ratios were >0.15 mmol/mol accompanied by relatively high Mg/Ca ratios (~4 mmol/mol)
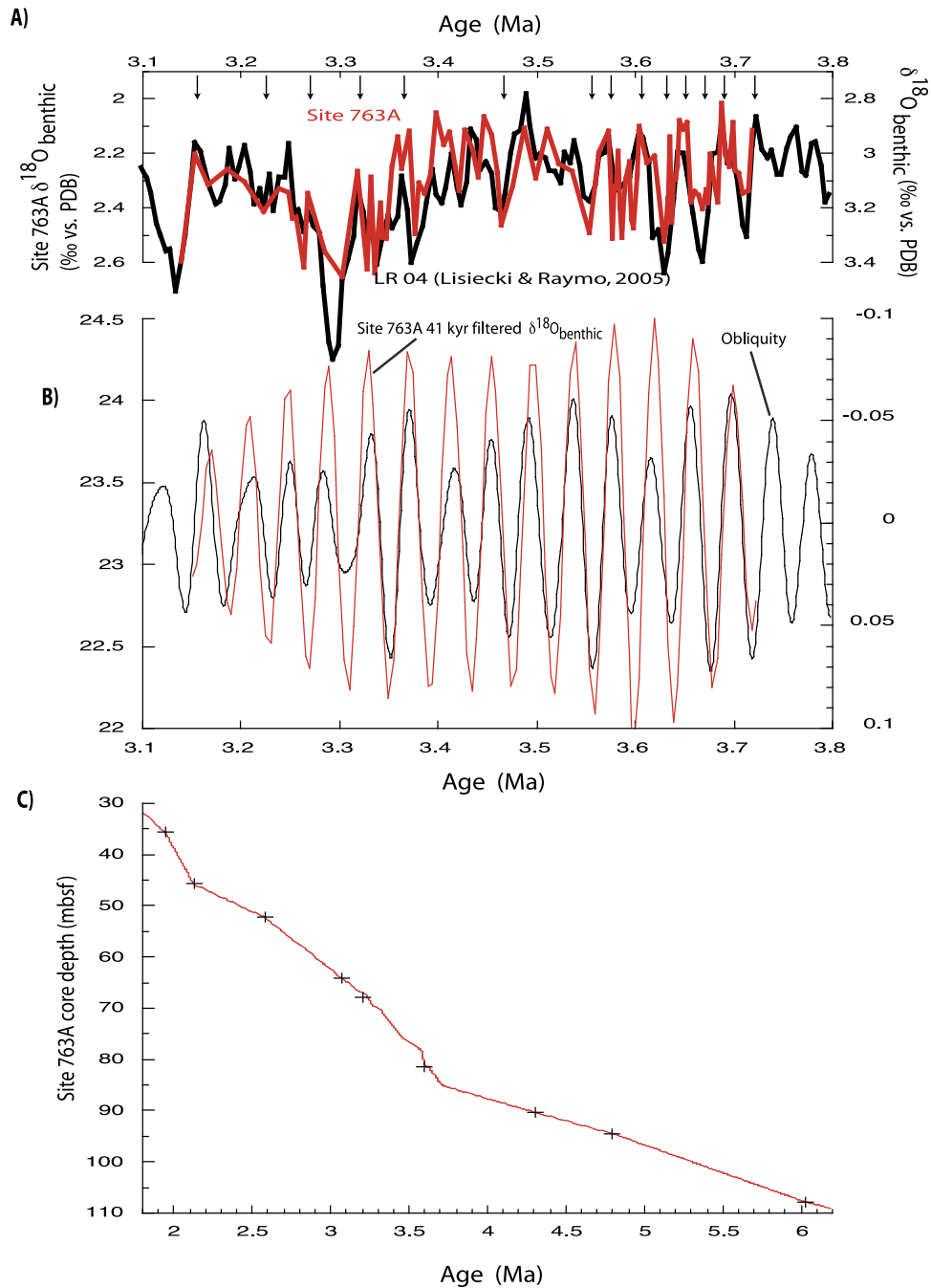
Figure 3. Stratigraphic framework of ODP Site 763A. (a) Tuning of the high-resolution benthic $\delta^{18}O_{C.\ wuellerstorfi}$ record (red line) to the global benthic reference stack LR04 (black line) [*Lisiecki and Raymo*, 2005]. Arrows indicate tie points. (b) The filtered 41 kyr component of the benthic $\delta^{18}O_{C.\ wuellerstorfi}$ record (red line) corrected for a 8 kyr phase lag being in accordance to the obliquity solution (black line) [*Laskar*, 1990]. (c) Diagram showing the age-depth relationship (red line) of Site 763A. Crosses indicate magnetic reversal datums [*Tang*, 1992; *Sinha and Singh*, 2008] that were updated to the ATNTS 2004 time scale [*Lourens et al.*, 2004].

which might be related to silicate contamination. For comparison with Mg/Ca derived temperature records from Site 214 [*Karas et al.*, 2009] the analysis of foraminiferal Mg/Ca ratios and the calculation of Mg/Ca temperatures are done consistently for all records shown in this study. Absolute differences in Mg/Ca data originating from the application of different Mg/Ca temperature calibrations or cleaning techniques (e.g., reductive cleaning) can hence be ruled out.

[8] Mg/Ca ratios of *G. sacculifer* were converted into temperatures by using the multispecies calibration of *Anand et al.* [2003]: Mg/Ca = 0.38 exp(0.09 × SST) with an accuracy of ±1.2°C. *G. sacculifer* is assumed to calcify in
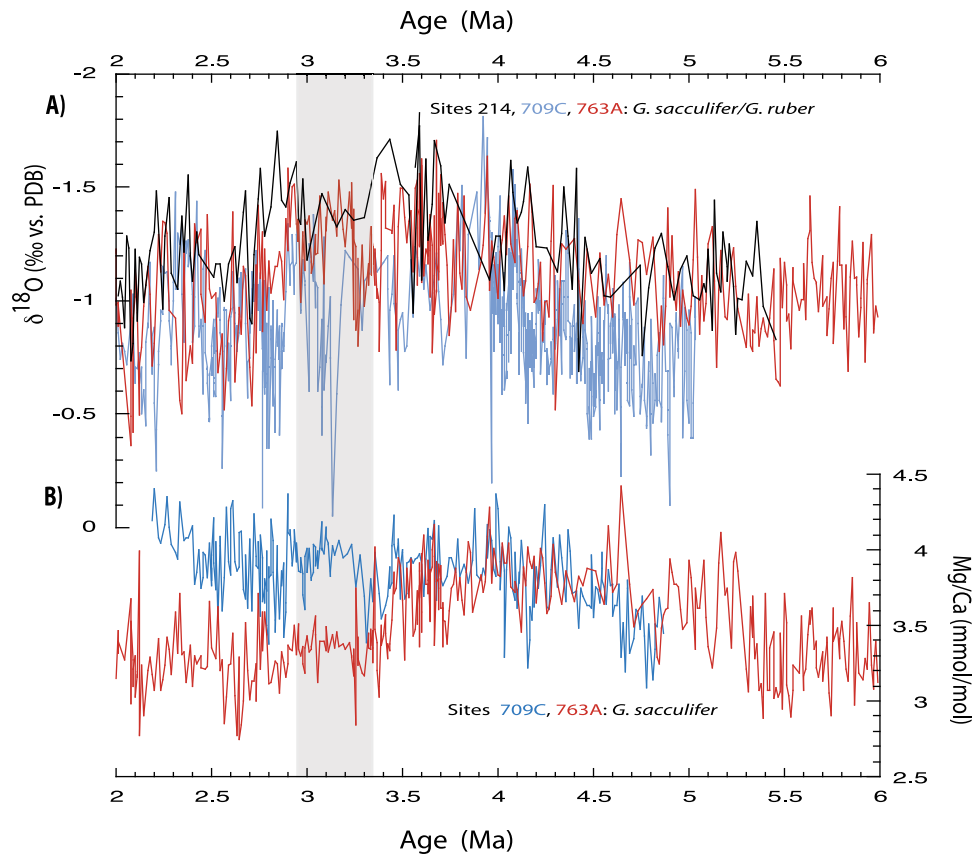
Figure 4. (a) Surface layer *G. ruber/G. sacculifer* δ^{18}O records from Site 214 (black line) [*Karas et al.*, 2009], Site 709C (blue line) [*Shackleton and Hall*, 1990], and Site 763A (red line, this study). (b) *G. sacculifer* Mg/Ca records from sites 763A (red line) and 709C (blue line) used to calculate surface temperatures. Note that Mg/Ca ratios from Site 709C were corrected after *Regenberg et al.* [2006] (see section 2.3).

the upper 50 m water depth [*Anand et al.*, 2003] and most likely records annual temperatures, as this shallow dwelling species occurs throughout the year in the tropics [*Lin et al.*, 2004].

2.3. Dissolution Effects on Pliocene Mg/Ca

[9] Calcite dissolution is the most critical issue for Mg/Ca thermometry, as Mg^{2+} is selectively removed from the foraminiferal tests [e.g., *Regenberg et al.*, 2006]. From core top studies, *Regenberg et al.* [2006] defined critical ΔCO_3^{2-} threshold values of ~20 μmol/kg, below which Mg^{2+} loss starts and proposed species-specific correction equations.

[10] Site 763A location (1367 m water depth) is situated well above the present lysocline in that region (deeper than ~3900 m) [*Martinez et al.*, 1999] and is above the critical ΔCO_3^{2-} level of ~20 μmol/kg (data from World Ocean Circulation Experiment transect 110 were used to calculate ΔCO_3^{2-} levels [*Lewis and Wallace*, 1998]). As *Haq et al.* [1990] and *Sinha et al.* [2006] also point to excellent foraminiferal preservation during the studied Pliocene time interval we decided not to correct the initial Mg/Ca values (Figure 4b). Instead, for Site 709C, we corrected the initial Mg/Ca data using the species-specific correction equation for *G. sacculifer* (Figure 4b) [*Regenberg et al.*, 2006], as modern ΔCO_3^{2-} values are on average at ~10 μmol/kg (data

from World Ocean Circulation Experiment transect 102E/W was used to calculate ΔCO_3^{2-} levels [*Lewis and Wallace*, 1998]) well below the critical threshold values. Nonetheless, Site 709C (3041 m water depth) is located above the present lysocline (~4400 m in the central tropical Indian Ocean [*Banakar et al.*, 1998]) and carbonates are well preserved throughout the studied time interval [*Backman et al.*, 1988].

[11] Possible temporal changes in calcite preservation affecting the Mg/Ca record are not defined in the applied dissolution correction. A significant change in calcite preservation, however, is not expected for the studied Pliocene time period at Site 709C. The $SST_{Mg/Ca}$ resemble those of the shallower Site 214, which are presumably not biased by dissolution [*Karas et al.*, 2009] and do not show distinct changes during the Pliocene which one would expect when preservation would have notably changed (Figure 5a). Relatively high and stable CaCO$_3$ contents of ~90% over the last 4 Myr [*Curry et al.*, 1990] support our notion. Even changes in the depth of the lysocline in the order of ~0.5 km as predicted by *Farrell and Prell* [1991] for the tropical Pacific over the last 4 Myr, would produce an error in Mg/Ca of ~5% [*Lea et al.*, 2000] when assuming a loss of ~12% in foraminiferal Mg/Ca per kilometer water depth [*Regenberg et al.*, 2006; *Dekens et al.*, 2002].
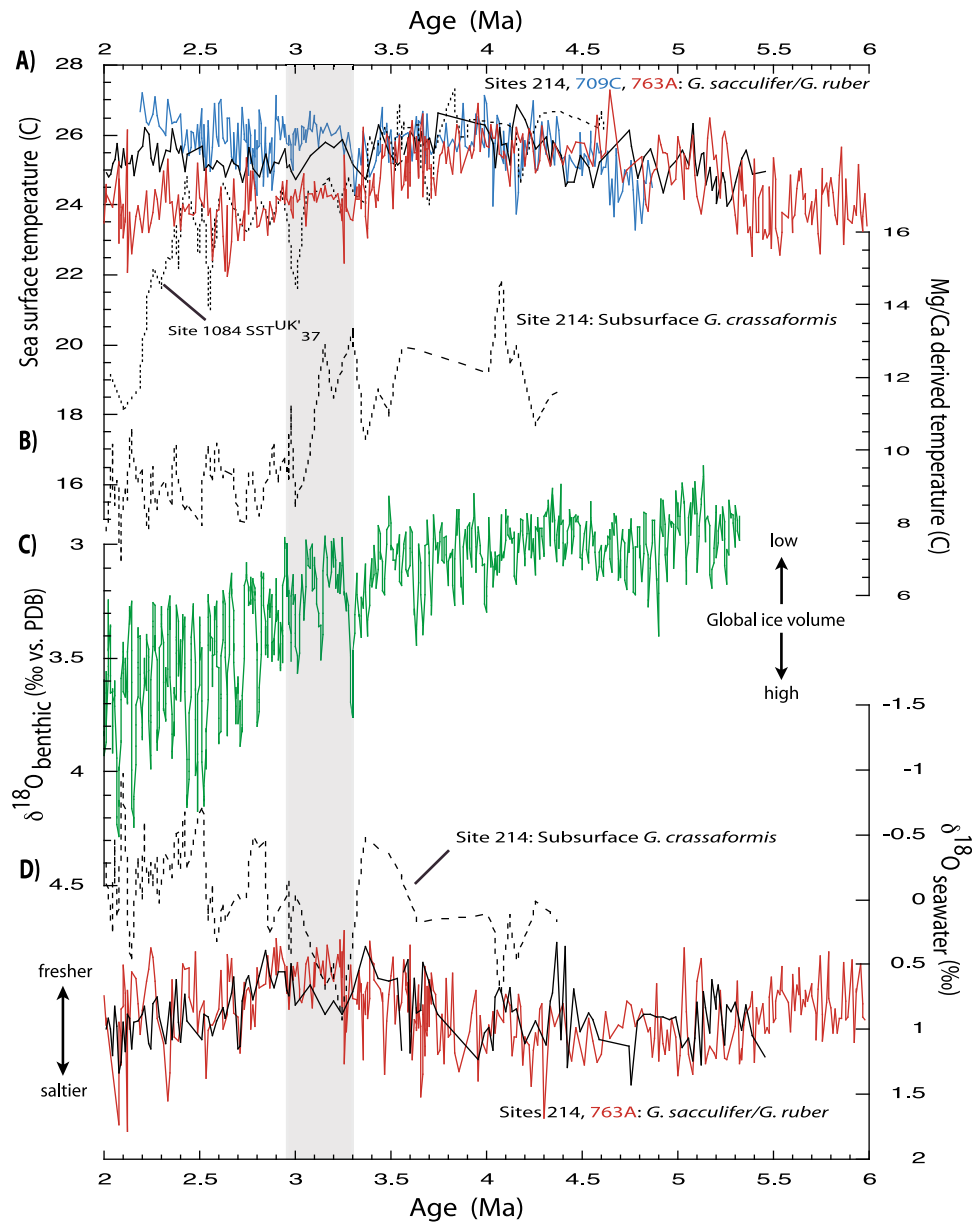
Figure 5. (a) *G. ruber/G. sacculifer* SST$_{Mg/Ca}$ from Site 214 (black line) [*Karas et al.*, 2009], Site 709C (blue, this study), Site 763A (red, this study), and alkenone-derived SST from Site 1084 in the Benguela upwelling system (dashed) [*Marlow et al.*, 2000; *Etourneau et al.*, 2009]. (b) *G. crassaformis* Mg/Ca-derived temperatures at the subsurface level from Site 214 (dashed) [*Karas et al.*, 2009]. (c) The LR04 global ice volume record from *Lisiecki and Raymo* [2005]. (d) *G. sacculifer* (Site 214, black; Site 763A, red) and subsurface *G. crassaformis* (Site 214, dashed) [*Karas et al.*, 2009] $\delta^{18}O_{seawater}$ records.

2.4. Calculation of $\delta^{18}O_{seawater}$

[12] To assess changes in ancient sea surface salinities, we used the combined $\delta^{18}O$ and Mg/Ca temperature [e.g., *Nürnberg*, 2000] records from the surface dwelling plank-tonic species *G. sacculifer*. The foraminiferal $\delta^{18}O$ signal is thereby dependent on global ice volume, salinity, and ocean temperature, whereas the foraminiferal Mg/Ca ratio is pre-dominantly determined by the ocean temperature. In accor-dance to *Karas et al.* [2009], we calculated $\delta^{18}O_{seawater}$ using the equation of *Shackleton* [1974], which reflects a combi-nation of ice volume controlled changes plus local variations

in $\delta^{18}O_{seawater}$ due to regional hydrological changes. We did not correct $\delta^{18}O_{seawater}$ for changes in the Pliocene global ice volume as $\delta^{18}O_{seawater}$ records from different core locations are equally influenced by variations in global ice volume. The resulting $\delta^{18}O_{seawater}$ values with an absolute error of ~±0.3‰ [*Schmidt*, 1999; *Rohling*, 2007] approximate rela-tive changes in salinity. The calculation of absolute paleo-SSS from $\delta^{18}O_{seawater}$ includes many assumptions, which are not always warranted. In particular, different ocean depths exhibit different salinity versus $\delta^{18}O_{seawater}$ relation-ships [e.g., *Regenberg et al.*, 2009]. Further, the observed

linear relationship between salinity and $\delta^{18}O_{seawater}$ most likely changed through time [*Rohling and Bigg*, 1998]. We hence remain interpreting the relative changes of $\delta^{18}O_{seawater}$ reflecting regional hydrological changes.

3. Results and Discussion

3.1. Development of Surface Hydrography

[13] The *G. ruber/G. sacculifer* $\delta^{18}O$ records of Site 709C from the tropical western Indian Ocean [*Shackleton and Hall*, 1990], of Site 763A from the subtropical eastern Indian Ocean, and of Site 214 from the tropical eastern Indian Ocean (Figure 4a) [*Karas et al.*, 2009] show similar long-term trends with decreasing values from the early Pliocene until ~3.5 Ma, changing toward more positive values during mid-Pliocene global cooling [*Ravelo et al.*, 2004]. However, absolute $\delta^{18}O$ values differ between cores. $\delta^{18}O$ values at Site 709C are commonly more positive than those at sites 214 and 763A, possibly indicating higher salinities there. Since ~3.5 Ma, $\delta^{18}O$ values at Site 763A start to deviate showing at times more positive values compared to Site 214. Foraminiferal Mg/Ca implies similar $SST_{Mg/Ca}$ during the early Pliocene at all sites with a long-term warming trend of ~2°C toward the mid-Pliocene at ~4–3.6 Ma (Figures 4b and 5a). This observation is in accordance with *Brierley et al.* [2009], who showed that during the early Pliocene the tropical warm pool was expanded with a reduced temperature gradient between the equator and the subtropics. During the mid-Pliocene, $SST_{Mg/Ca}$ from the tropical western Indian Ocean Site 709C remained stable at ~26°C (Figure 5a) and broadly resemble those from tropical eastern Indian Ocean Site 214 [*Karas et al.*, 2009]. The long-term decrease of ~1°C, which is evident at sites 214 and 806 [*Wara et al.*, 2005; *Karas et al.*, 2009], is not seen at Site 709C implying that the tropical western Indian Ocean might have been less influenced by mid-Pliocene global cooling [*Ravelo et al.*, 2004]. From ~3.3 Ma onward, $SST_{Mg/Ca}$ at Leeuwin Current Site 763A became significantly cooler by 2–3°C than at tropical sites 214 and 709C from the present-day Indian Ocean Warm Pool. This gradient in $SST_{Mg/Ca}$ is comparable to modern conditions with an annual SST difference of ~2°C between sites [*Locarnini et al.*, 2006], implying that present-day SST conditions were already reached during the mid-Pliocene.

[14] Within the critical time period at 3.5–3 Ma, when we register a different hydrographic development at the ocean surface between sites 214 and 763A, there is evidence for distinct tectonic induced changes in the subsurface level (~300–450 m water depth) *G. crassaformis* Mg/Ca derived temperatures and $\delta^{18}O_{seawater}$ (Figures 1, 5a, 5b, 5d) [*Karas et al.*, 2009] at tropical eastern Indian Ocean Site 214. The observation of more saline subsurface conditions during ~3.3–3.1 Ma at Site 214 (Figure 5d) was interpreted as a consequence of the tectonic reorganization of the Indonesian Gateway [*Karas et al.*, 2009]. Either the contribution of cooler and fresher ITF waters to this site was reduced and replaced by warmer and saltier tropical Indian Ocean waters or a switch back to more warm and saline South Pacific source waters occurred [*Karas et al.*, 2009]. After ~2.95 Ma, the change in ITF subsurface waters from a South to a dominant North Pacific source finalized [*Karas et al.*, 2009] indicated by fresher and cooler conditions at the subsurface level at Site 214 (Figures 5b and 5d).

3.2. Pliocene Changes in the Leeuwin Current and Indian Ocean Polar Heat Transport

[15] It is important to note, however, that at Site 763A the surface ocean definitely cooled before the switch of ITF source waters finalized at ~2.95 Ma. Surface cooling began at ~3.5 Ma, and after ~3.3 Ma the impact of warm tropical waters diminished compared to the tropical eastern and western Indian Ocean sites 214 and 709C (Figure 5a). At the same time, subsurface waters at Site 214 became more saline in line with a reduction of the ITF (Figure 5d) [*Karas et al.*, 2009]. Both, the more saline conditions at the subsurface level at Site 214 and the cooler surface conditions at Site 763A suggest a significant reduction of the ITF at 3.3–3.1 Ma. As today the Leeuwin Current is controlled mainly by the ITF [e.g., *Feng et al.*, 2003], we suspect that it was clearly reduced during the mid-Pliocene when the ITF declined due to the new tectonic setting in the Indonesian Gateway [*Cane and Molnar*, 2001; *Gaina and Müller*, 2007]. We presuppose in this respect that the Leeuwin Current was present also during the mid-Pliocene indicated by *G. sacculifer* $\delta^{18}O_{seawater}$ records from sites 214 and 763A, which are very similar and imply a common ITF source water (Figure 5d).

[16] In fact, various modeling studies pointed out the effects of the mid-Pliocene ITF reduction [*Hirst and Godfrey*, 1993; *Godfrey*, 1996; *Lee et al.*, 2002]. With an entirely closed Indonesian Gateway, these models generate scenarios quite similar to our reconstructions. Our observed $SST_{Mg/Ca}$ pattern in the Indian Ocean suggests a weaker Leeuwin Current being ~2°C cooler, while $SST_{Mg/Ca}$ at the tropical eastern and western Indian Ocean sites 214 and 709C remain rather stable. In this respect, a cooling of surface ITF waters during this time interval causing the $SST_{Mg/Ca}$ decline in the Leeuwin Current area seems rather unlikely as the $SST_{Mg/Ca}$ at Site 214 (and at Site 806) [*Wara et al.*, 2005] are hardly changing (Figure 5a) [*Karas et al.*, 2009]. We therefore consider the reduction in ITF and not just a cooling as causative for the cooling at Leewin Current Site 763A. This notion is further supported by tectonic reconstructions of the ITF region, which propose a shoaling of the Indonesian Gateway with the emergence of small islands like Timor [*Cane and Molnar*, 2001; *Gaina and Müller*, 2007; *Kuhnt et al.*, 2004], and in consequence, a restricted throughflow [*Kuhnt et al.*, 2004].

[17] The tectonic reorganization might indeed have reduced the surface throughflow volume since ~3.3 Ma, whereas the subsurface ITF after ~3.1 Ma again started to cool and freshen due to the switch to North Pacific source waters [*Karas et al.*, 2009]. This switch might have supported the surface layer cooling of Site 763A through mixing processes of the cold and fresh subsurface waters from the Indonesian region [*Hirst and Godfrey*, 1993; *Song and Gordon*, 2004]. In contrast, changes in the monsoon systems (Indian and Asian monsoon), driving oceanographic changes in that area today and possibly on glacial-interglacial timescales [*Gordon et al.*, 2003; *Xu et al.*, 2008], are unlikely of having cooled the (sub)surface during the mid-Pliocene time period ~3.5–3 Ma, when Indonesian surface and subsurface flow changed. Significant changes in the monsoon systems and in South China SST clearly appeared after 3 Ma [*Gupta and Thomas*, 2003; *Jia et al.*, 2008].

[18] Our findings of a reduced Leeuwin Current are consistent with marine and terrestrial palynological studies off northwestern Australia and from southwestern Australia, respectively [*Martin and McMinn*, 1994; *Dodson and Macphail*, 2004]. These studies suggest the expansion of aridity around 3 Ma in the southwest, the disappearance of rain forest and the development of shrub/grasslands in northwestern Australia. Indeed cooler SST in that area through a reduced Leeuwin Current would have caused a significant reduction in precipitation in the coastal areas of western and southwestern Australia [*Feng et al.*, 2003].

[19] Apart from climatic effects on western Australia, we observe from 3.5 to 3 Ma a similar surface layer cooling at Site 1084 in the Benguela upwelling system [*Marlow et al.*, 2000] as we registered at Site 763A (Figure 5a). Both temperature records show an almost identical development until 2.4 Ma, when alkenone-derived SST from Site 1084 further drops significantly. The good match of both SST records until late Pliocene times supports our notion that the restriction of the Indonesian Gateway possibly contributed to the cooling of the Benguela upwelling system [*Karas et al.*, 2009]. Such cooling most likely resulted not only from the proposed cooling of subsurface waters in the tropical eastern Indian Ocean [*Karas et al.*, 2009], but also from the reduced surface throughflow of Indonesian waters. Support comes from modeling studies [*Hirst and Godfrey*, 1993; *Godfrey*, 1996], which suggest both a weaker Leeuwin Current when the ITF is closed, and a weaker Agulhas Current resulting in a significant surface cooling of ~1°C of the Agulhas outflow region close to Site 1084. In consequence, the poleward heat flux in the Indian Ocean would have been considerably reduced [*Hirst and Godfrey*, 1993; *Gordon*, 2005] explaining the enhanced meridional temperature gradient in the Indian Ocean and the cooling of the Benguela upwelling system during a time of global warmth with reduced meridional temperature gradients [*Brierley et al.*, 2009]. After ~2.4 Ma, the significant cooler alkenone SST at Site 1084 compared to the SST$_{Mg/Ca}$ at Site 763A are most likely related to the intensification of the trade winds and marked cooling of the Southern Ocean, which initiated the modern-like Benguela upwelling system (Figure 5a) [*Etourneau et al.*, 2009]. At the same time, SST$_{Mg/Ca}$ at Site 763A remained relatively warm caused by a still flowing Leeuwin Current. Even though it was cooler and/or reduced, it prevented strong coastal upwelling, which would likely have developed without the presence of the Leeuwin current [*Smith et al.*, 1991; *Morrow et al.*, 2003].

4. Conclusions

[20] We reconstructed the Pliocene surface hydrography of the tropical western and subtropical eastern Indian Ocean. During the critical time period ~3.5–2.95 Ma of the restriction of the Indonesian Gateway, Ocean surface temperatures from the eastern and western tropical Indian Ocean sites 214 [*Karas et al.*, 2009] and 709C remained rather constant, while those at Site 763A significantly dropped, being since ~3.3 Ma 2–3°C cooler than the tropical sites. This implies a reduced Leeuwin Current inline to significant tectonic induced changes in the subsurface level at Site 214 [*Karas et al.*, 2009]. Hence, we suggest that the tectonic restriction of the Indonesian Gateway led to a reduced surface ITF, which considerably weakened the Leeuwin Current since ~3.3 Ma. Most likely, this reduced surface ITF with a weakened Leeuwin Current led to a diminished poleward heat transport, possibly resulting in a cooling of the Benguela upwelling system.

References

Anand, P., H. Elderfield, and M. H. Comte (2003), Calibration of Mg/Ca thermometry in planktonic foraminifera from a sediment trap time series, *Paleoceanography*, 18(2), 1050, doi:10.1029/2002PA000846.

Antonov, J. I., R. A. Locarnini, T. P. Boyer, A. V. Mishonov, and H. E. Garcia (2006), *World Ocean Atlas 2005*, vol. 2, *Salinity*, *NOAA Atlas NESDIS*, vol. 62, edited by S. Levitus, 182 pp., NOAA, Silver Spring, Md.

Backman, J., et al. (1988), Site 709, *Proc. Ocean Drill. Program Initial Rep.*, 115, 459–588.

Banakar, V. K., G. Parthiban, and P. Jauhari (1998), Chemistry of surface sediments along a north-south transect across the equator in the central Indian basin: An assessment of biogenic and detrital influences on elemental burial on the seafloor, *Chem. Geol.*, 147, 217–232, doi:10.1016/S0009-2541(98)00015-1.

Barker, S., M. Greaves, and H. Elderfield (2003), A study of cleaning procedures used for foraminiferal Mg/Ca paleothermometry, *Geochem. Geophys. Geosyst.*, 4(9), 8407, doi:10.1029/2003GC000559.

Brierley, C. M., A. V. Fedorov, Z. Liu, T. D. Herbert, K. T. Lawrence, and J. P. LaRiviere (2009), Weakened Hadley circulation and greatly expanded tropical warm pool in the Early Pliocene, *Science*, 323, 1714–1718, doi:10.1126/science.1167625.

Cane, M., and P. Molnar (2001), Closing of the Indonesian seaway as a precursor to east African aridification around 3–4 million years ago, *Nature*, 411, 157–162, doi:10.1038/35075500.

Curry, W. B., J. L. Cullen, and J. Backman (1990), Carbonate accumulation in the Indian Ocean during the Pliocene: Evidence for a change in productivity and preservation at about 2.4 Ma, *Proc. Ocean Drill. Program Sci. Results*, 115, 509–518.

Dekens, P. S., D. W. Lea, D. K. Pak, and H. J. Spero (2002), Core top calibration of Mg/Ca in tropical foraminifera: Refining paleotemperature estimation, *Geochem. Geophys. Geosyst.*, 3(4), 1022, doi:10.1029/2001GC000200.

Dodson, J. R., and M. K. Macphail (2004), Palynological evidence for aridity events and vegetation change during the Middle Pliocene, a warm period in Southwestern Australia, *Global Planet. Change*, 41, 285–307, doi:10.1016/j.gloplacha.2004.01.013.

Elderfield, H., M. Vautravers, and M. Cooper (2002), The relationship between shell size and Mg/Ca, Sr/Ca, $\delta^{18}O$, and $\delta^{13}C$ of species of planktonic foraminifère, *Geochem. Geophys. Geosyst.*, 3(8), 1052, doi:10.1029/2001GC000194.

Etourneau, J., P. Martinez, T. Blanz, and R. Schneider (2009), Pliocene-Pleistocene variability of upwelling activity, productivity, and nutrient cycling in the Benguela Region, *Geology*, 37, 871–874, doi:10.1130/G25733A.1.

Farrell, J. W., and W. L. Prell (1991), Pacific CaCO$_3$ Preservation and $\delta^{18}O$ since 4Ma: Paleoceanic and Paleoclimatic Implications, *Paleoceanography*, 6, 485–498, doi:10.1029/91PA00877.

Feng, M., G. Meyers, A. Pearce, and S. Wijffels (2003), Annual and interannual variations of the Leeuwin Current at 32°S, *J. Geophys. Res.*, 108(C11), 3355, doi:10.1029/2002JC001763.

Gaina, C., and D. Müller (2007), Cenozoic tectonic and depth/age evolution of the Indonesian gateway and associated back-arc basins, *Earth Sci. Rev.*, 83, 177–203, doi:10.1016/j.earscirev.2007.04.004.

Godfrey, J. S. (1996), The effect of the Indonesian Throughflow on ocean circulation and heat exchange with the atmosphere: A review, *J. Geophys. Res.*, 101, 12,217–12,237, doi:10.1029/95JC03860.

Gordon, A. L. (2005), Oceanography of the Indonesian Seas and their throughflow, *Oceanography*, 18(4), 14–27.

Gordon, A. L., R. D. Susanto, and K. Vranes (2003), Cool Indonesian throughflow as a consequence of restricted surface layer flow, *Nature*, 425, 824–828, doi:10.1038/nature02038.

Gupta, A. K., and E. Thomas (2003), Initiation of Northern Hemisphere glaciation and strengthening of the northeast Indian monsoon: Ocean drilling program site 758, eastern equatorial Indian Ocean, *Geology*, *31*, 47–50, doi:10.1130/0091-7613(2003)031<0047:IONHGA>2.0.CO;2.

Haq, B. U., et al. (1990), Site 763, *Proc. Ocean Drill. Program Initial Rep.*, *122*, 289–352.

Hirst, A. C., and J. S. Godfrey (1993), The role of Indonesian Throughflow in a Global Ocean GCM, *J. Phys. Oceanogr.*, *23*, 1057–1086, doi:10.1175/1520-0485(1993)023<1057:TROITI>2.0.CO;2.

Jia, G., F. Chen, and P. Peng (2008), Sea surface temperature differences between the western equatorial Pacific and northern South China Sea since the Pliocene and their paleoclimatic implications, *Geophys. Res. Lett.*, *35*, L18609, doi:10.1029/2008GL034792.

Karas, C., D. Nürnberg, A. K. Gupta, R. Tiedemann, K. Mohan, and T. Bickert (2009), Mid-Pliocene climate change amplified by a switch in Indonesian subsurface throughflow, *Nat. Geosci.*, *2*, 434–438, doi:10.1038/ngeo520.

Kuhnt, W., A. Holbourn, R. Hall, M. Zuvela, and R. Käse (2004), Neogene history of the Indonesian Throughflow, in *Continent-Ocean Interactions in the East Asian Marginal Seas*, *Geophys. Monogr. Ser.*, vol. 149, edited by P. D. Clift et al., p. 299–320, Washington, D. C.

Laskar, J. (1990), The chaotic motion of the solar system: A numerical estimate of the chaotic zones, *Icarus*, *88*, 266–291, doi:10.1016/0019-1035 (90)90084-M.

Lea, D. W., D. K. Pak, and H. J. Spero (2000), Climate impact of Late Quaternary equatorial Pacific sea surface temperature variations, *Science*, *289*, 1719–1724, doi:10.1126/science.289.5485.1719.

Lee, T., I. Fukumori, D. Menemenlis, Z. Xing, and L. L. Fu (2002), Effects of the Indonesian Throughflow on the Pacific and Indian oceans, *J. Phys. Oceanogr.*, *32*, 1404–1429, doi:10.1175/1520-0485(2002)032<1404: EOTITO>2.0.CO;2.

Lewis, E., and D. W. R. Wallace (1998), Program developed for CO_2 system calculations, *Rep. ORNL/CDIAC-105*, Carbon Dioxide Inf. Anal. Cent., Oak Ridge Natl. Lab., U.S. Dep. of Energy, Oak Ridge, Tenn.

Lin, H.-L., W.-C. Wang, and G.-W. Hung (2004), Seasonal variation of planktonic foraminiferal isotopic composition from sediment traps in the South China Sea, *Mar. Micropaleontol.*, *53*, 447–460, doi:10.1016/ j.marmicro.2004.08.004.

Lisiecki, L. E., and M. E. Raymo (2005), A Pliocene-Pleistocene stack of 57 globally distributed benthic $\delta^{18}O$ records, *Paleoceanography*, *20*, PA1003, doi:10.1029/2004PA001071.

Locarnini, R. A., A. V. Mishonov, J. I. Antonov, T. P. Boyer, and H. E. Garcia (2006), *World Ocean Atlas 2005*, vol. 1, *Temperature*, *NOAA Atlas NESDIS*, vol. 61, edited by S. Levitus, 182 pp., NOAA, Silver Spring, Md.

Lourens, L. J., et al. (2004), Appendix 2: Orbital tuning calibrations and conversions for the Neogene Period, in *A Geologic Time Scale 2004*, edited by F. M. Gradstein, J. G. Ogg, and A. G. Smith, pp. 469–484, Cambridge Univ. Press, Cambridge, U. K.

Marlow, J. R., C. B. Lange, G. Wefer, and A. Rosell-Melé (2000), Upwelling intensification as part of the Pliocene-Pleistocene climate transition, *Science*, *290*, 2288–2291.

Martin, H. A., and A. McMinn (1994), Late Cainozoic vegetation history of north-western Australia, from the palynology of a deep sea core (ODP Site 765), *Aust. J. Bot.*, *42*, 95–102, doi:10.1071/BT9940095.

Martinez, J. I., P. De Deckker, and T. T. Barrows (1999), Palaeoceanography of the last glacial maximum in the eastern Indian Ocean: Planktonic foraminiferal evidence, *Palaeogeogr. Palaeoclimatol. Palaeoecol.*, *147*, 73–99, doi:10.1016/S0031-0182(98)00153-9.

Morrow, R., F. Fang, M. Fieux, and R. Molcard (2003), Anatomy of three warm-core Leeuwin Current eddies, *Deep Sea Res., Part II*, *50*, 2229–2243, doi:10.1016/S0967-0645(03)00054-7.

Mudelsee, M., and M. E. Raymo (2005), Slow dynamics of the Northern Hemisphere glaciation, *Paleoceanography*, *20*, PA4022, doi:10.1029/ 2005PA001153.

Nürnberg, D. (2000), Taking the temperature of past ocean surfaces, *Science*, *289*, 1698–1699, doi:10.1126/science.289.5485.1698.

Paillard, D., L. Labeyrie, and P. Yiou (1996), Macintosh program performs time-series analysis, *Eos Trans. AGU*, *77*, 379, doi:10.1029/96EO00259.

Ravelo, A. C., D. H. Andreasen, M. Lyle, A. O. Lyle, and M. W. Wara (2004), Regional climate shifts caused by gradual global cooling in the Pliocene epoch, *Nature*, *429*, 263–267, doi:10.1038/nature02567.

Regenberg, M., D. Nürnberg, S. Steph, J. Groeneveld, D. Garbe-Schönberg, R. Tiedemann, and W.-C. Dullo (2006), Assessing the effect of dissolution on planktonic foraminiferal Mg/Ca ratios: Evidence from Caribbean core tops, *Geochem. Geophys. Geosyst.*, *7*, Q07P15, doi:10.1029/2005GC001019.

Regenberg, M., S. Steph, D. Nürnberg, R. Tiedemann, and D. Garbe-Schönberg (2009), Calibrating Mg/Ca ratios of multiple planktonic foraminiferal species with $\delta^{18}O$-calcification temperatures: Paleothermometry for the upper water column, *Earth Planet. Sci. Lett.*, *278*, 324–336, doi:10.1016/j.epsl.2008.12.019.

Rohling, E. J. (2007), Progress in paleosalinity: Overview and presentation of a new approach, *Paleoceanography*, *22*, PA3215, doi:10.1029/ 2007PA001437.

Rohling, E. J., and G. R. Bigg (1998), Paleosalinity and $\delta^{18}O$: A critical assessment, *J. Geophys. Res.*, *103*, 1307–1318, doi:10.1029/97JC01047.

Schmidt, G. (1999), Error analysis of paleosalinity calculations, *Paleoceanography*, *14*, 422–429, doi:10.1029/1999PA900008.

Shackleton, N. J. (1974), Attainment of isotope equilibrium between ocean water and the benthonic foraminiferal genus Uvigerina. Isotopic changes in the ocean during the last glacial, *Colloq. Int. C. N. R. S.*, *219*, 203–209.

Shackleton, N. J., and M. A. Hall (1990), Pliocene oxygen isotope stratigraphy of Hole 709C, *Proc. Ocean Drill. Program Sci. Results*, *115*, 529–538.

Sinha, D. K., and A. K. Singh (2008), Late Neogene planktic foraminiferal biochronology of the ODP Site 763A, Exmouth Plateau, southeast Indian Ocean, *J. Foraminiferal Res.*, *38*, 251–270, doi:10.2113/gsjfr.38.3.251.

Sinha, D. K., A. K. Singh, and M. Tiwari (2006), Paleoceanographic and palaeoclimatic history of ODP site 763A (Exmouth Plateau), southeast Indian Ocean: 2.2 Ma record of planktic foraminifera, *Curr. Sci.*, *90*, 1363–1369.

Smith, R. L., A. Huyer, J. S. Godfrey, and J. A. Church (1991), The Leeuwin Current off western Australia 1986–87, *J. Phys. Oceanogr.*, *21*, 323–345, doi:10.1175/1520-0485(1991)021<0323:TLCOWA>2.0.CO;2.

Song, Q., and A. L. Gordon (2004), Significance of the vertical profile of the Indonesian Throughflow transport to the Indian Ocean, *Geophys. Res. Lett.*, *31*, L16307, doi:10.1029/2004GL020360.

Talley, L. (2003), Shallow, intermediate, and deep overturning components of the global heat budget, *J. Phys. Oceanogr.*, *33*, 530–560, doi:10.1175/ 1520-0485(2003)033<0530:SIADOC>2.0.CO;2.

Tang, C. (1992), Paleomagnetism of Cenozoic sediments in Holes 762B and 763A, Central Exmouth Plateau, northwest Australia, *Proc. Ocean Drill. Program Sci. Results*, *122*, 717–733.

Tiedemann, R., A. Sturm, S. Steph, S. P. Lund, and J. Stoner (2007), Astronomically calibrated timescales from 6 to 2.5 Ma and benthic isotope stratigraphies, Sites 1236, 1237, 1239, and 1241, *Proc. Ocean Drill. Program Sci. Results*, *202*, 1–69, doi:10.2973/odp.proc.sr.202.210.2007.

Wara, M. W., A. C. Ravelo, and M. L. Delaney (2005), Permanent El Niño-like conditions during the Pliocene Warm Period, *Science*, *309*, 758–761, doi:10.1126/science.1112596.

Xu, J., A. Holbourn, W. Kuhnt, Z. Jian, and H. Kawamura (2008), Changes in the thermocline structure of the Indonesian outflow during Terminations I and II, *Earth Planet. Sci. Lett.*, *273*, 152–162, doi:10.1016/j. epsl.2008.06.029.

D. Garbe-Schönberg, Institute of Geosciences, University of Kiel, D-24118 Kiel, Germany.

C. Karas, Goethe-University Frankfurt, Altenhoeferallee 1, D-60438, Frankfurt am Main, Germany. (karas@em.uni-frankfurt.de)

D. Nürnberg, Leibniz Institute of Marine Sciences (IFM-GEOMAR), University of Kiel, Wischhofstrasse 1-3, D-24148 Kiel, Germany.

R. Tiedemann, Alfred Wegener Institute for Polar and Marine Research, Am Alten Hafen 26, D-27568 Bremerhaven, Germany.